Antenna Radiation Pattern Measurement in a Nonanechoic Chamber

Saulo M. Fróes, Pablo Corral, Marcela S. Novo, Miguel Aljaro, and Antônio C. de C. Lima

***Abstract*—Several techniques are being studied with the objective of recovering the real antenna radiation patterns through measurements performed in nonanechoic environments. This is being proven by the use of digital signal processing techniques, based on several concepts, such as deconvolution, impulse response, and filtering. In this letter, a new methodology to obtain the actual antenna radiation patterns in noisy environments is proposed. An algorithm was developed that identifies similar points (power/angle) of the antenna radiation patterns through repeated measurements in different directions. Then, the most similar points were chosen, and the radiation pattern of the antenna was reconstructed and compared with the radiation pattern of the same antenna obtained in an anechoic chamber. The results demonstrate that the proposed technique is promising in the reconstruction of radiation pattern of antennas in noisy environments.**

***Index Terms*—Antenna measurements, nonanechoic measurements site, radiation pattern.**

I. Introduction

THE determination of antenna radiation patterns can be a complex and exhaustive task. To determine the fundamental parameters of antennas and their radiation characteristics, an alternative is the use of numerical methods, which in some cases offer acceptable results. However, measurements of the antenna radiation pattern are crucial to validate the numerical results and corroborate the design of new and modern antennas.

It is well known that measurements of antenna radiation patterns are preferably carried out in anechoic chambers. Such chambers are characterized by their ability to reduce reflections of electromagnetic waves in an attempt to simulate the free-space environment. However, the cost of an anechoic chamber is directly related to its size and the quality of its absorbers, which makes it impossible for many small companies and research centers to acquire them.

A recent research focus is on the reduction of error in the measurements of the fundamental parameters of antennas performed in nonanechoic or semianechoic chambers. From research in this area, some strategies have already been developed to retrieve the actual antenna radiation pattern. One of these is based on the fast Fourier transform (FFT-based method) [1], [2]. The FFT technique has proved to be quite efficient, but it requires the previous knowledge of the environment for determining the direct path, which is not a simple task to perform. To overcome this problem, another method proposes the use of angular deconvolution [3], a recent experimental technique that does not need *a priori* knowledge of the measurement site. The work in [4] presented a technique of echo suppressing using multiprobe antennas to collect several measurements and resolve the direct contribution of the antenna under test (AUT). However, this method only works if the AUT is in a fixed direction during the tests. The works in [5] and [6] investigated the spatial mode filtering approach, based on the expansion of the measured data in a set of spherical wave functions combined with a modal filtering. Another technique uses the matrix pencil algorithm for reconstructing the radiation pattern, as described in [7]–[9]. The advantages of this technique are the possibility of measurements at narrower frequency steps, lower processing requirements, and lack of prior knowledge of the measurement environment. There is also a strategy using the frequency impulse response of the nonanechoic chamber [10], [11]. This method is limited to antenna measurements with dimensions similar to those used to obtain impulse response from the measurement site. The Hilbert transform (HT) is another technique of radiation patterns retrieval [12], [13]. This method is similar to the FFT-based one, and it works without phase measurement. However, the HT can only be used if the direct path power is greater than the sum of the power of all other paths in order to meet the minimum phase criterion, which may fail in some cases.

All the above-mentioned papers have introduced techniques for reconstructing the antenna radiation pattern obtained in nonanechoic sites. However, they work for specific conditions, providing an opportunity to seek a more general solution. The technique proposed in this letter consists of measuring the antenna radiation pattern in different spatial positions and identifying the most significant points of gain or attenuation due to reflections or external interference. For accomplishing that, an algorithm was developed to compare the measured data, point to point, and discard the ones with the greater discrepancy. Then, the reconstructed radiation pattern is composed by a weighted average of the most similar points. The experimental results of antenna radiation patterns in a noisy environment are then reconstructed with the technique proposed here, and these are compared with the radiation patterns of the same antennas obtained in an anechoic chamber, showing a very good agreement.

Manuscript received November 27, 2018; revised December 18, 2018; accepted December 23, 2018. Date of publication January 9, 2019; date of current version February 1, 2019. *(Corresponding author: Saulo M. Fróes.)*

S. M. Fróes, M. S. Novo, and A. C. de C. Lima are with the Mechatronics Post Graduation Program and the Department of Electrical Engineering, Federal University of Bahia, Salvador 40170-115, Brazil (e-mail: saulo.froes@ibge.gov.br; marcela.novo@ufba.br; acdcl@ufba.br).

P. Corral and M. Aljaro are with the Department of Communications Engineering and the Department of Physics and Computers Architecture, Miguel Hernández University, 03202 Elche, Spain (e-mail: pcorral@umh.es; aljaro@umh.es).

Digital Object Identifier 10.1109/LAWP.2019.2891972

Fig. 1. Nonanechoic measurement room.

II. Measurement System

Measurements of the antenna radiation characteristics were carried out at the Miguel Hernández University's Electronic Technology Laboratory. The room used in the experiments was not designed for measurements of antenna radiation patterns, as it does not have any RF signal absorber or isolator. In addition, inside the room, there are furniture and electronic devices that can act as reflectors and sources of active noise. Fig. 1 shows this nonanechoic environment.

The measurement setup consists of a transmitter antenna fixed to a static base, as shown in Fig. 1, and an AUT attached to a step motor controlled by an Arduino. A horn-type transmitting antenna with operating frequencies equal to 2.4 and 5.3 GHz was used. At the reception, a Yagi–Uda antenna and a horn antenna were used for comparison purposes. The Yagi–Uda and Horn antennas were chosen because they represent two different classes of antennas (linear and aperture). In addition, these antennas are frequently used for many applications.

All the antenna radiation patterns presented in this letter are E-plane patterns, and they represent the directivity of the antennas. The proposed technique is analogous to H-plane patterns. In our study, antenna gain and efficiency were not measured because this would require a more complex measurement system.

III. Results

The antennas were arranged in three different positions in the nonanechoic room, and three measurements were taken for each position. Thus, three average radiation patterns were calculated, reducing the effect of temporary sources of RF noise or even errors due to mechanical vibrations. Fig. 2 shows the arrangements of the measurement setup. The data were then processed using signal processing techniques. Basically, two stages of signal processing were performed: alignment and filtering.

Due to mechanical limitations, it was necessary to align the curves since the antennas were not perfectly aligned before the measurements. Thus, the cross-correlation algorithm was used to find the ideal angle change to align the curves. This procedure was used for both curves measured in the same position and for curves measured at different positions.

The filtering technique used was the locally weighted regression and the dispersion graph smoothing (LOWESS). It was necessary to filter the signal to eliminate high-frequency noise, making the curves smoother.

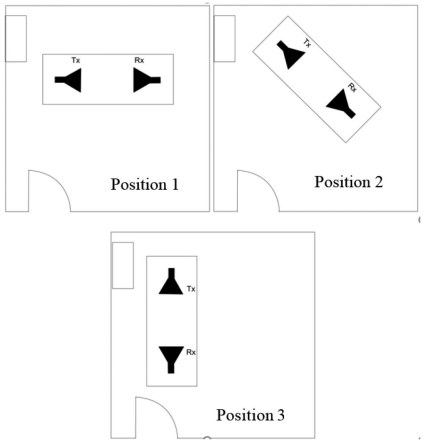

Fig. 2. Arrangement of the antennas during the measurements.

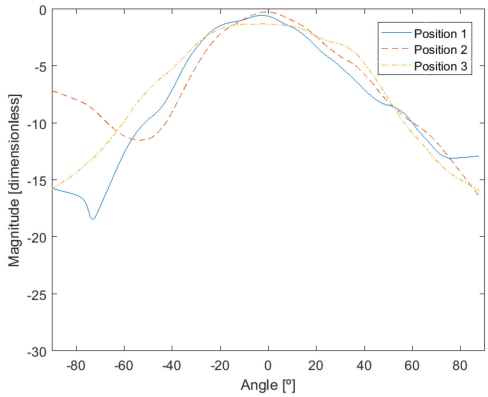

Fig. 3. Radiation pattern diagrams of a Yagi–Uda antenna operating at 2.4 GHz.

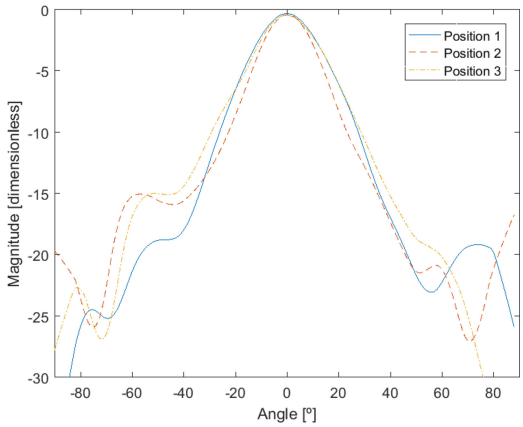

Fig. 4. Radiation pattern diagrams of a horn antenna operating at 5.3 GHz

Fig. 3 shows the measured radiation patterns of a Yagi–Uda antenna operating at 2.4 GHz. Fig. 4 illustrates the measured radiation patterns of a horn antenna operating at 5.3 GHz. It should be noted that, in both cases, the results presented are obtained after the alignment and filtering stages.

From these results, it can be noted that there are differences between the radiation patterns of the measured antenna, depending on the position of the measurement system. This is because of the existence of reflections and sources of noise in the room, which can influence the radiation pattern on a larger or smaller scale.

IV. Retrieving the Antenna Radiation Pattern

The proposed technique to retrieve the actual radiation pattern from the measurements made is presented in the following. To analyze the results, the radiation patterns of the AUTs were measured in an anechoic chamber. Therefore, the errors calculated here refer to differences related to the measurement performed in the anechoic chamber.

The algorithm elaborated for retrieving the actual pattern can be summarized in the following three steps.

1) For each angle (α), compare the three patterns and determine the biggest [$B(\alpha)$], smallest [$S(\alpha)$], and medium [$M(\alpha)$] values.
2) Determine if $M(\alpha)$ is closer to $B(\alpha)$ or $S(\alpha)$. Two variables are used for rating how close it is from $B(\alpha)$ and $S(\alpha)$.
3) If $M(\alpha)$ is closer to $B(\alpha)$, a new point is calculated for the retrieval curve closer to $M(\alpha)$ and $B(\alpha)$ than $S(\alpha)$. However, if $M(\alpha)$ is closer to $S(\alpha)$, the new point will be closer to $M(\alpha)$ and $S(\alpha)$ than $B(\alpha)$. This step is executed through a weighted average using the rates calculated in step two.

To calculate the weighted average weights used in step 3 above, it is necessary to initially calculate two variables that represent, in percentage, how close is $M(\alpha)$ to $B(\alpha)$ ($p(\alpha)$) and how close is $M(\alpha)$ to $S(\alpha)$ ($q(\alpha)$). $p(\alpha)$ and $q(\alpha)$ can be determined by using the following:

$$p(\alpha) = 1 - \frac{B(\alpha) - M(\alpha)}{B(\alpha) - S(\alpha)} \tag{1}$$

$$q(\alpha) = 1 - \frac{M(\alpha) - S(\alpha)}{B(\alpha) - S(\alpha)}. \tag{2}$$

After p and q obtained, the weights were calculated as follows:

$$w_1(\alpha) = e^{p(\alpha)-0.5} \tag{3}$$

$$w_2(\alpha) = e^{q(\alpha)-0.5}. \tag{4}$$

It should be noted that the above-mentioned relations were established through exhaustive empirical tests. The retrieved radiation pattern diagram is obtained after calculating the retrieved point [RP(α)] for $\alpha = 0$ to $\alpha = 179$. The RP(α) is given as follows:

$$\mathrm{RP}(\alpha) = \frac{w_1(\alpha) \times \frac{B(\alpha)+M(\alpha)}{2} + w_2(\alpha) \times \frac{M(\alpha)+S(\alpha)}{2}}{w_1(\alpha) + w_2(\alpha)}. \tag{5}$$

A. Results for a Yagi–Uda Antenna at 2.4 GHz

Fig. 5 illustrates the retrieved pattern, as well as the patterns that were measured in the nonanechoic room. All patterns are in linear scale and normalized. These patterns were compared with the ones measured in the anechoic room. Fig. 5 also illustrates a curve that represents the error (difference between the curves).

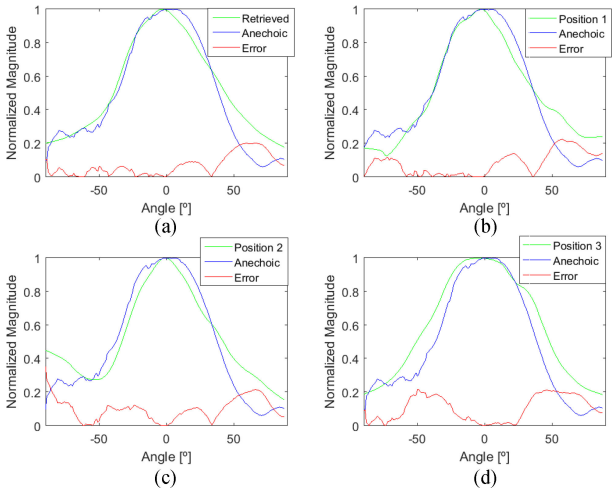

Fig. 5. Retrieved radiation patterns compared with the measured pattern in an anechoic chamber. (a) Retrieved. (b) Position 1. (c) Position 2. (d) Position 3. A Yagi–Uda antenna operating at 2.4 GHz.

TABLE I
Errors for a Yagi–Uda Antenna @ 2.4 GHz

Yagi-Uda – 2.4 GHz				
	MSE	**Standard Deviation**	**Maximum Error**	**HPBW**
Position 1	0.0113110	0.068139	0.22566	76.475°
Position 2	0.0147390	0.068035	0.35544	75.615°
Position 3	0.0165170	0.075889	0.21596	99.186°
Retrieved	0.0086319	0.061867	0.20248	83.025°
Anechoic	-	-	-	75.606°

Anechoic versus nonanechoic measurements.

Table I shows the mean square error (MSE), the standard deviation, and the maximum error for each curve compared with the anechoic chamber measurement. There are improvements in the three parameters that are analyzed. The improvements obtained with the recovered pattern reached about 47% for the MSE, 18% for the standard deviation, and 43% for the maximum error. Table I also presents the half-power beamwidth (HPBW) of the antenna. Although the HPBW obtained from the retrieved pattern is about 10% greater than the anechoic chamber, it is 68% closer to it than the HPBW of the position 3. In other words, if the radiation pattern was only measured with the antennas in the position 3 (worst case), the HPBW would be 68% worse than the retrieved one. The measurement of positions 1 and 2 has shown an HPBW closer to that the anechoic one, which is always possible to happen. The HPBW of the retrieved pattern from the anechoic one was influenced by the position 3 measurement. However, it was in a smaller scale than the positions 1 and 2 influences, which corroborates with the algorithm idea.

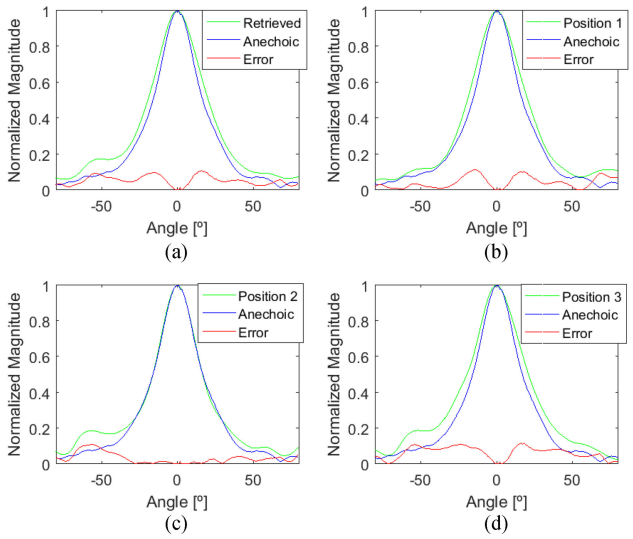

Fig. 6. Retrieved radiation patterns compared with the measured pattern in an anechoic chamber. (a) Retrieved. (b) Position 1. (c) Position 2. (d) Position 3. Horn antenna operating at 5.3 GHz.

TABLE II
ERRORS FOR A HORN ANTENNA @ 5.3 GHZ

Horn Antenna – 5.3 GHz				
	MSE	**Standard Deviation**	**Maximum Error**	**HPBW**
Position 1	0.0027078	0.031829	0.11324	40.119°
Position 2	0.0025214	0.033795	0.15112	32.747°
Position 3	0.0046935	0.034028	0.11641	40.888°
Retrieved	0.0032373	0.025037	0.10794	39.964°
Anechoic	-	-	-	33.104°

Anechoic versus nonanechoic measurements.

B. Results for a Horn Antenna at 5.3 GHz

Analogously, Fig. 6 brings the results, and Table II shows the errors for the measurements with a horn antenna operating at 5.3 GHz. From Table II, it can be noted that the MSE of the retrieved pattern was smaller than the position 3 measurements by about 31%. For the standard deviation and maximum error, the retrieved pattern presented the smallest values, reaching a maximum improvement of 26% and 28%, respectively.

The values of the HPBW are shown in the last column of Table II. The retrieved HPBW value was closer to the anechoic one when compared with the measurements at positions 1 and 3. When compared with the measurements at position 3, the worst case, the retrieved HPBW value was about 11% closer to the anechoic one.

V. CONCLUSION

An approach was presented in this letter for reconstruction of the real radiation pattern diagram of an antenna, when measurements are carried out in nonanechoic chambers. The results showed the efficiency of the technique, which proved to be capable to reduce the effects of the most accentuated reflections/attenuations, when they occurred in a specific position.

It is important to highlight that the retrieved pattern is not guaranteed to be the best one, when compared with all the measurements taken. For example, if a measured pattern is quite close to the anechoic one, other measurements with worse results can negatively influence the retrieved radiation pattern. For this technique to work efficiently, anomalies due to reflections should not be found in the same region of the antenna pattern for different measurement positions. Whenever this condition is achieved, it is possible to identify and correct these anomalies through the presented algorithm.

The proposed technique reached its main objective since universities, small companies, and research centers can apply it to obtain radiation diagrams with a greater chance of error reduction due to reflections without the need of an anechoic chamber. Further work can be done through the evaluation of the effectiveness of the proposed technique with other classes of antennas.

REFERENCES

[1] G. Le Fur *et al.*, "Improvement of antenna measurement results at low frequencies by using post-processing techniques," in *Proc. 8th Eur. Conf. Antennas Propag.*, The Hague, Netherlands, 2014, pp. 1680–1684.
[2] J. Koh, A. De, T. K. Sarkar, H. Moon, W. Zhao, and M. S. Palma, "Free space radiation pattern reconstruction from non-anechoic measurements using an impulse response of the environment," *IEEE Trans. Antennas Propag.*, vol. 60, no. 2, pp. 821–831, Feb. 2012.
[3] M. Spirlet, C. Geuzaine, and V. Beauvois, "Experimental correction of radiation patterns between electromagnetic environments," *IEEE Trans. Antennas Propag.*, vol. 65, no. 3, pp. 1330–1338, Mar. 2017.
[4] K. A. Yinusa and T. F. Eibert, "A multi-probe antenna measurement technique with echo suppression capability," *IEEE Trans. Antennas Propag.*, vol. 61, no. 10, pp. 5008–5016, Oct. 2013.
[5] L. J. Foged *et al.*, "Echo suppression by spatial-filtering techniques in advanced planar and spherical near-field antenna measurements [AMTA Corner]," *IEEE Antennas Propag. Mag.*, vol. 55, no. 5, pp. 235–242, Oct. 2013.
[6] T. Kozan, S. Burgos, L. J. Foged, F. Saccardi, and P. O. Iversen, "Comparison of a direct low-pass filtering technique with spherical modal filtering applied to the suppression of range reflections in antenna measurements," in *Proc. 8th Eur. Conf. Antennas Propag.*, The Hague, Netherlands, 2014, pp. 2481–2485.
[7] P. González-Blanco and M. Sierra-Castañer, "Time filtering techniques for echo reduction in antenna measurements," in *Proc. 10th Eur. Conf. Antennas Propag.*, Davos, Switzerland, 2016, pp. 1–3.
[8] P. González-Blanco and M. Sierra-Castañer, "Analysis of time filtering techniques for echo reduction in antenna measurements," *Int. J. Microw. Wireless Technol.*, vol. 9, no. 7, pp. 1387–1395, 2017.
[9] G. León, S. Loredo, S. Zapatero, and F. E. Las Heras, "Radiation pattern error corrections based on matrix pencil method," in *Proc. IEEE Antennas Propag. Soc. Int. Symp.*, 2008, pp. 1–4.
[10] C. Segura, W. Cho, J. Jeon, and J. Koh, "Free space radiation pattern reconstruction from non-anechoic data using the 3d impulse response of the environment," *Prog. Electromagn. Res. M*, vol. 73, pp. 37–46, 2018.
[11] H. Moon, T. S. Sarkar, and W. Zhao, "Reconstruction of three-dimensional free space radiation pattern using non-anechoic measurements factored by the impulse response of the environment," in *Proc. IEEE Conf. Antenna Meas. Appl.*, 2016, pp. 1–4.
[12] S. Loredo, G. Leon, R. G. Ayestaran, and F. Las-Heras, "Reconstruction of antenna radiation patterns from phaseless measurements in nonanechoic chambers," *IEEE Antennas Wireless Propag. Lett.*, vol. 10, pp. 1282–1285, 2011.
[13] D. Cassioli and E. A. Mecozzi, "Minimum-phase impulse response channels," *IEEE Trans. Commun.*, vol. 57, no. 12, pp. 3529–3532, Dec. 2009.